

Supplementary Information

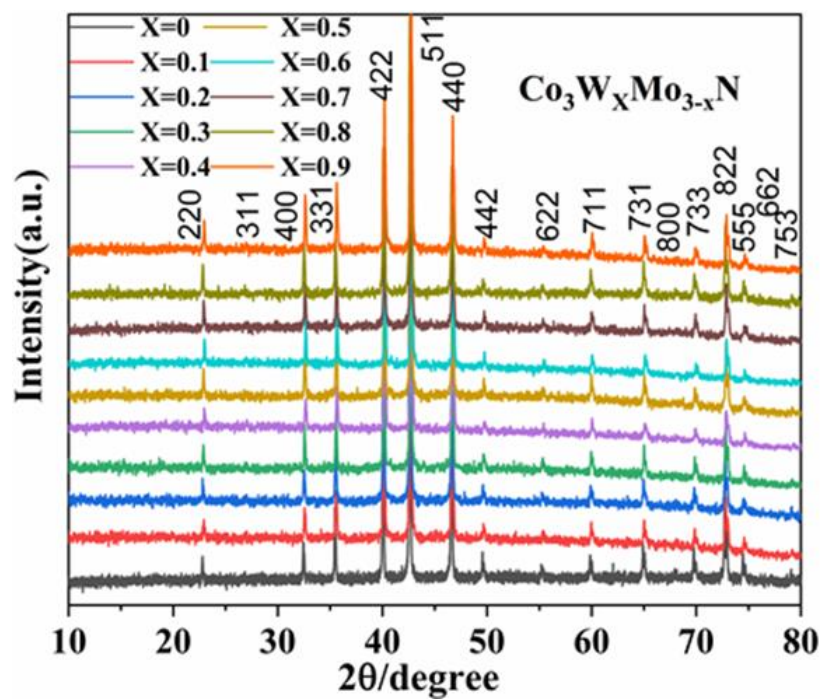


Fig. S1 XRD patterns of $\text{Co}_3\text{W}_x\text{Mo}_{3-x}\text{N}$ ($x = 0.0, 0.1, 0.2, 0.3, 0.4, 0.5, 0.6, 0.7, 0.8$ and 0.9) samples heated under NH_3 at 900°C for 12 h.

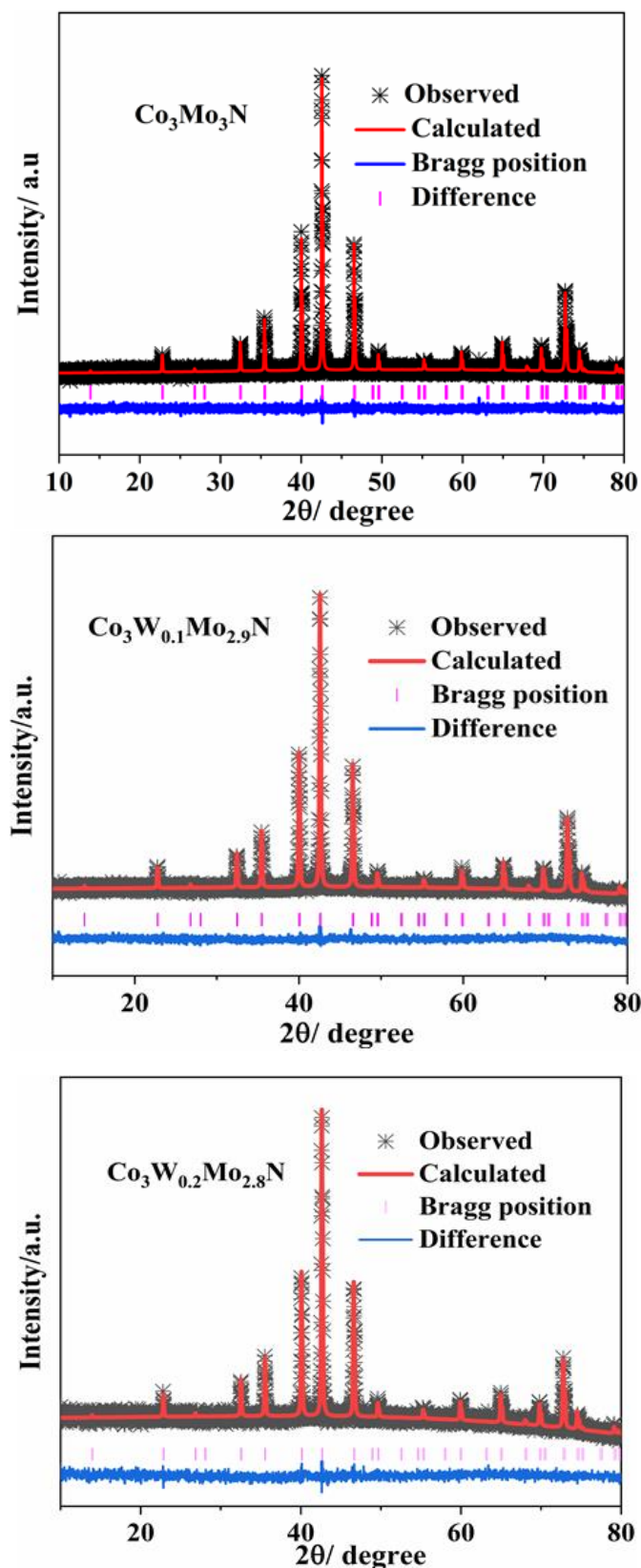


Fig. S2 Rietveld fits to the XRD patterns of $\text{Co}_3\text{W}_x\text{Mo}_{3-x}\text{N}$ series, where $x = 0$; ($R_{\text{wp}} \% = 3.9$ and $R_p \% = 3.13$), 0.1 ; ($R_{\text{wp}} \% = 4.9$ and $R_p \% = 3.9$) and 0.2 ; ($R_{\text{wp}} \% = 4.9$ and $R_p \% = 3.9$). Black crosses mark the data points, the red continuous line the fit and the blue continuous line the difference. Pink tick marks show the positions of the allowed reflections for the η -carbide structure $\text{Co}_3\text{W}_x\text{Mo}_{3-x}\text{N}$ series in space group $Fd\bar{3}m$.

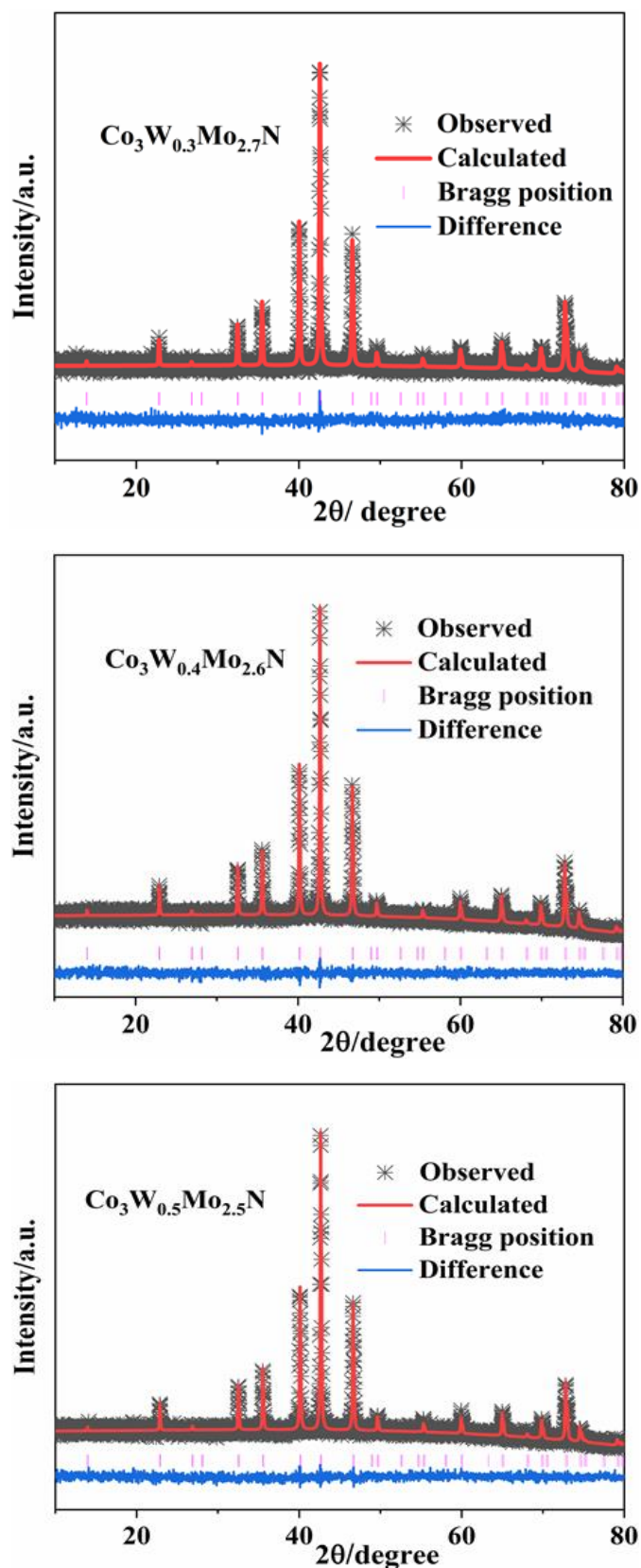


Fig. S3 Rietveld fits to the XRD patterns of $\text{Co}_3\text{W}_x\text{Mo}_{3-x}\text{N}$ series, where $x = 0.3$; ($R_{\text{wp}} \% = 4.9$ and $R_{\text{p}} \% = 3.9$), and 0.4 ; ($R_{\text{wp}} \% = 4.73$ and $R_{\text{p}} \% = 3.9$) and 0.5 ; ($R_{\text{wp}} \% = 4.9$ and $R_{\text{p}} \% = 3.9$). The data points and Rietveld fits are overlaid in black crosses and red line, respectively. The difference plots are shown in blue. The pink tick marks represent the allowed reflection position for $\text{Co}_3\text{W}_x\text{Mo}_{3-x}\text{N}$ series with space group $Fd\bar{3}m$.

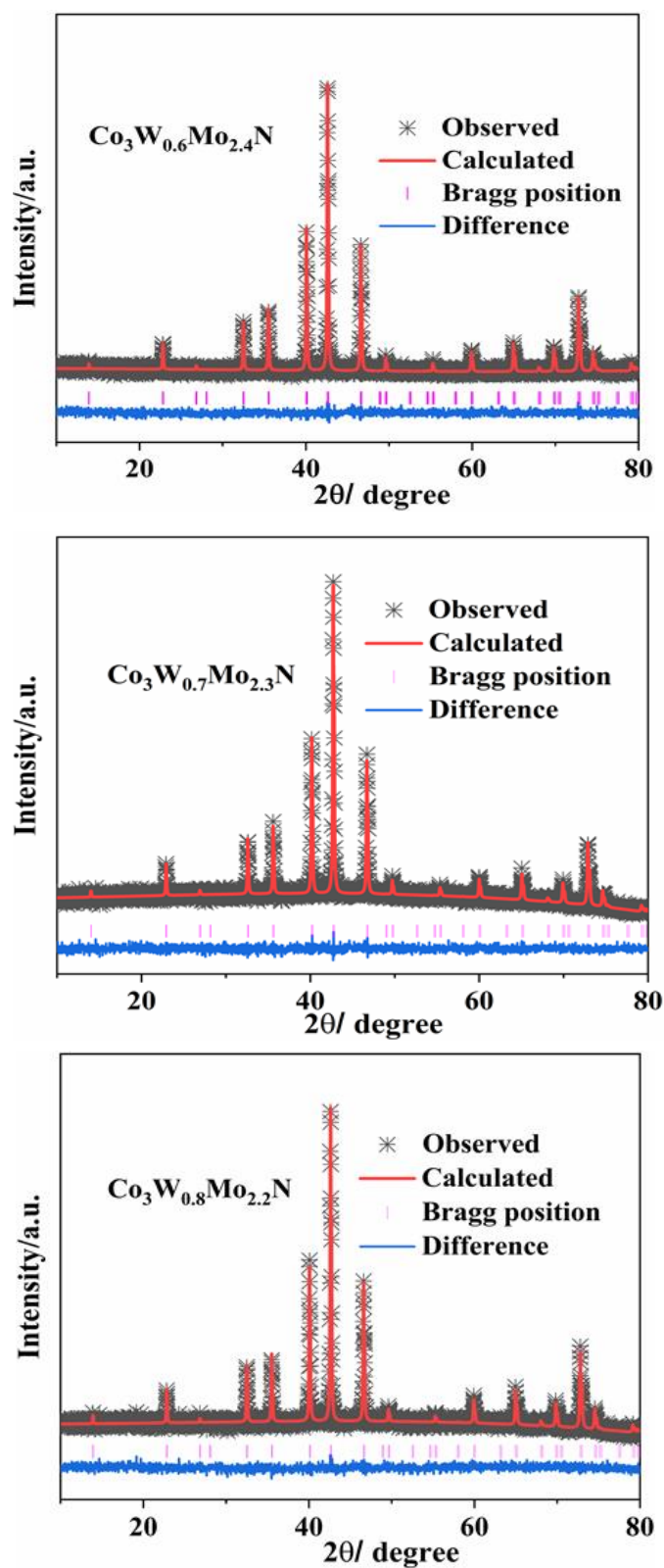


Fig. S4 Rietveld fits to the XRD patterns of $\text{Co}_3\text{W}_x\text{Mo}_{3-x}\text{N}$ series, where $x = 0.6$; ($R_{\text{wp}} \% = 5.03$ and $R_{\text{p}} \% = 4$), 0.7 ; ($R_{\text{wp}} \% = 5.3$ and $R_{\text{p}} \% = 4.18$) and 0.8 ; ($R_{\text{wp}} \% = 5.2$ and $R_{\text{p}} \% = 4.08$). Black crosses mark the data points, the red continuous line the fit and the blue continuous line the difference. Pink tick marks show the positions of the allowed reflections for the η -carbide structure $\text{Co}_3\text{W}_x\text{Mo}_{3-x}\text{N}$ series in space group $Fd\bar{3}m$.

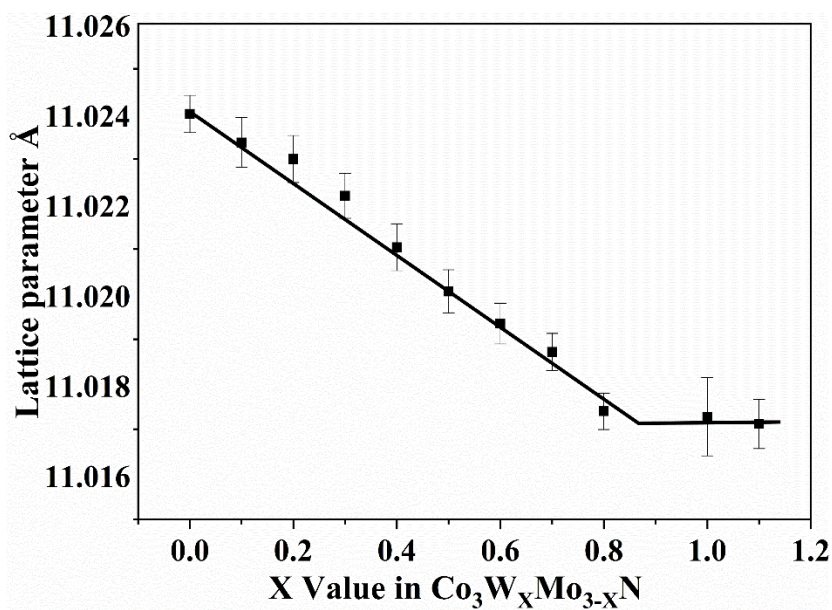


Fig. S5 Lattice parameter variation with tungsten content for $\text{Co}_3\text{W}_x\text{Mo}_{3-x}\text{N}$ samples, showing the limit of tungsten solubility just above $x = 0.8$.

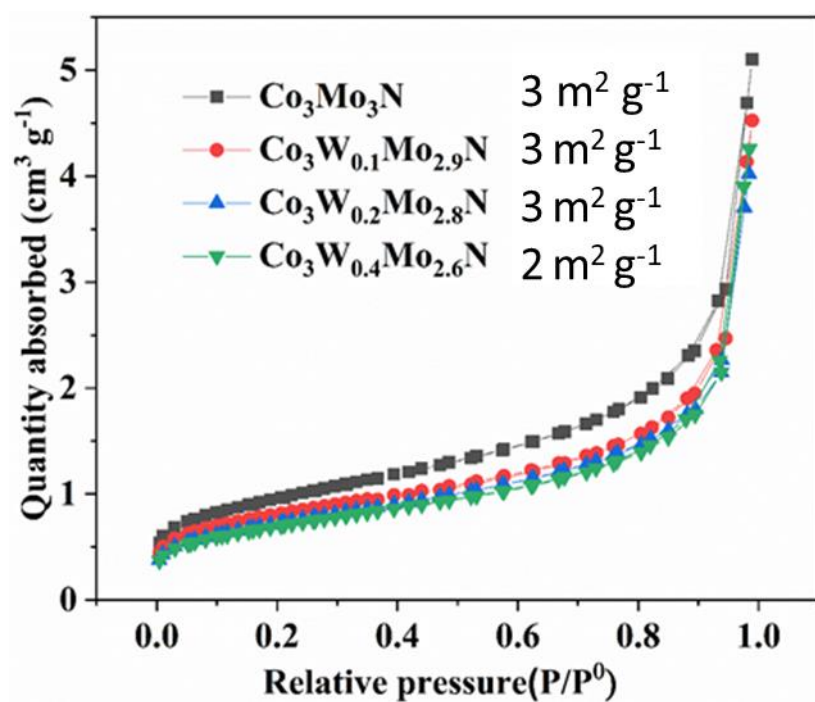


Fig. S6 Nitrogen adsorption/desorption isotherm curves for the $\text{Co}_3\text{W}_x\text{Mo}_{3-x}\text{N}$ samples.

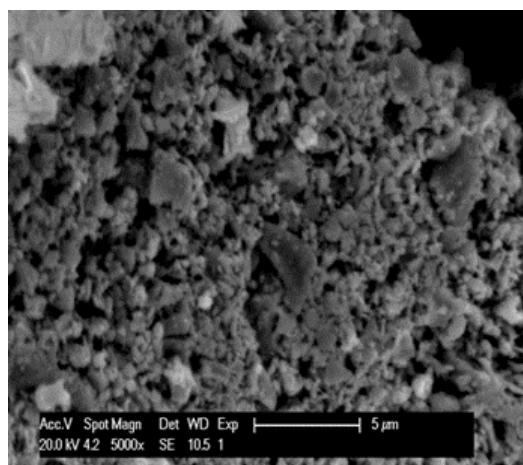


Fig. S7 Representative SEM image of $\text{Co}_3\text{Mo}_{2.6}\text{W}_{0.4}\text{N}$.

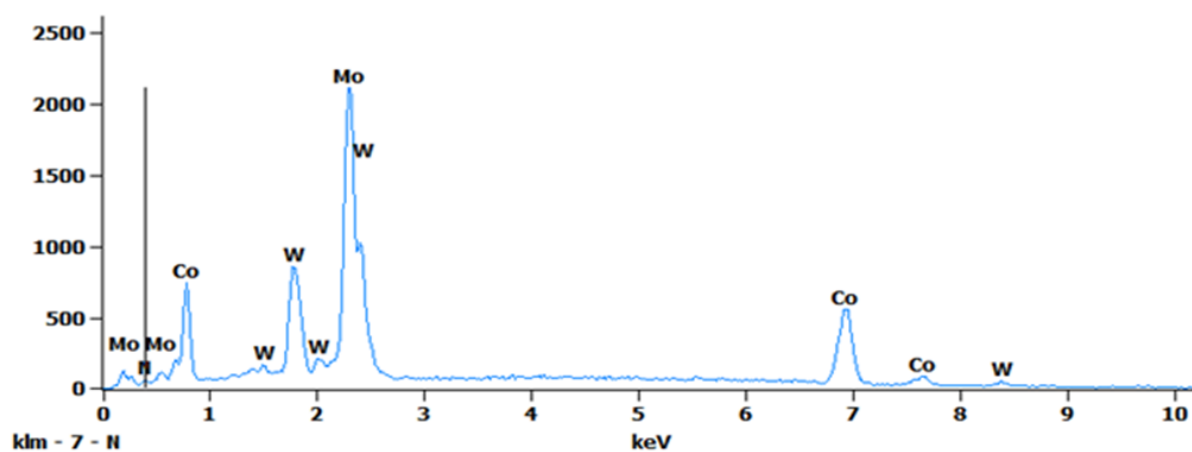


Fig. S8 EDX analysis for nanostructured $\text{Co}_3\text{Mo}_{2.6}\text{W}_{0.4}\text{N}$ using a 15 kV accelerating voltage.

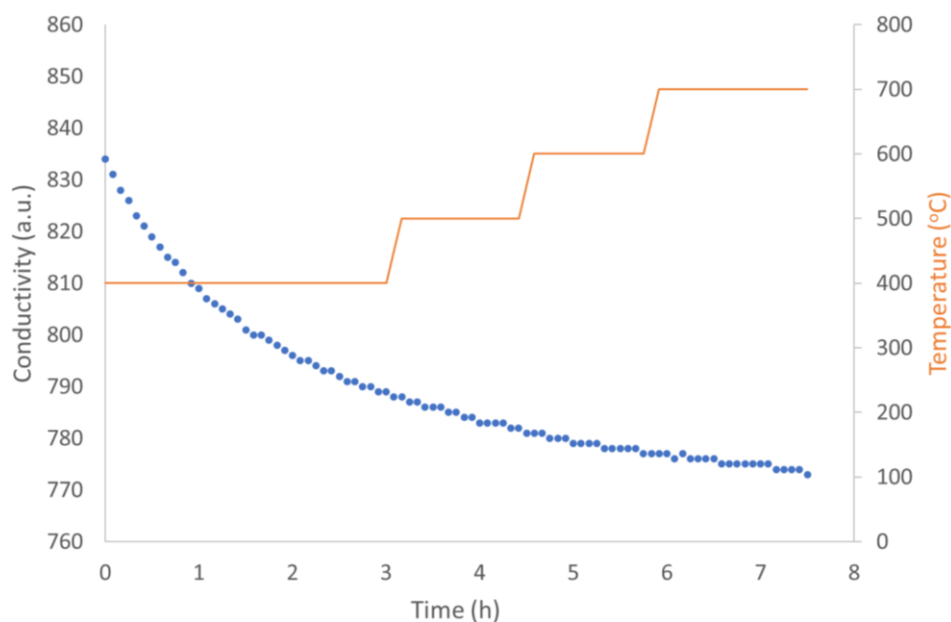


Fig. S9 Reaction profile of $\text{Co}_3\text{Mo}_3\text{N}$ under 3:1 H_2/Ar at 400°C for 3 h, 500°C for 1 h 15 min, 600°C for 1 h 10 min and 700°C for 1 h 35 min. Conductivity relates to that of aqueous sulfuric acid solution through which the reactor effluent is flowed. Decreasing conductivity corresponds to ammonia production wherein H^+ ions react with NH_3 to form NH_4^+ ions.

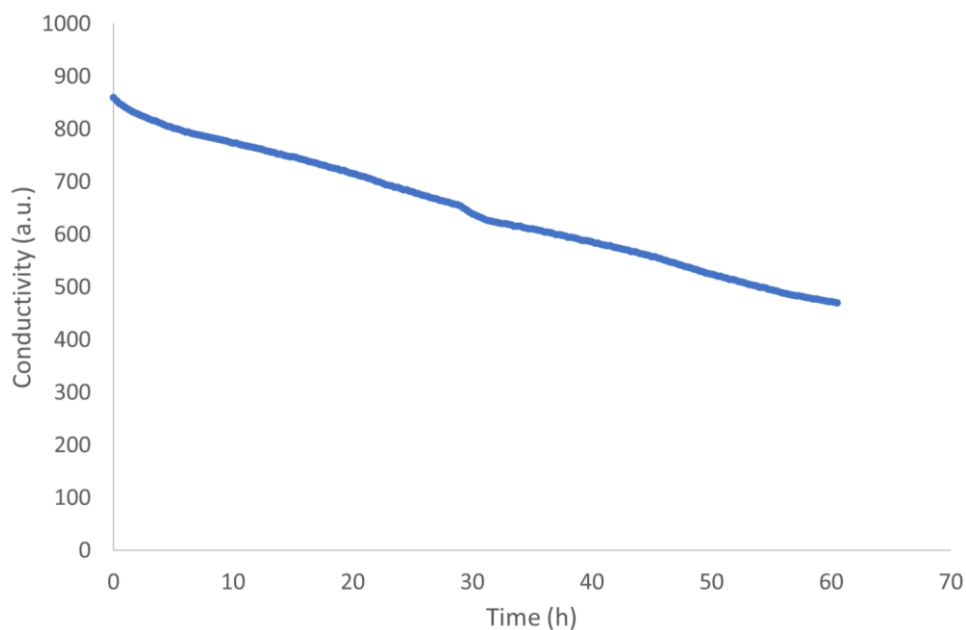


Fig. S10 Reaction profile of $\text{Co}_3\text{Mo}_{2.6}\text{W}_{0.4}\text{N}$ under 3:1 H_2/N_2 at 400°C for 60.5 h. The flask of dilute sulfuric acid was changed at 30 h. Conductivity relates to that of aqueous sulfuric acid solution through which the reactor effluent is flowed. Decreasing conductivity corresponds to ammonia production wherein H^+ ions react with NH_3 to form NH_4^+ ions.

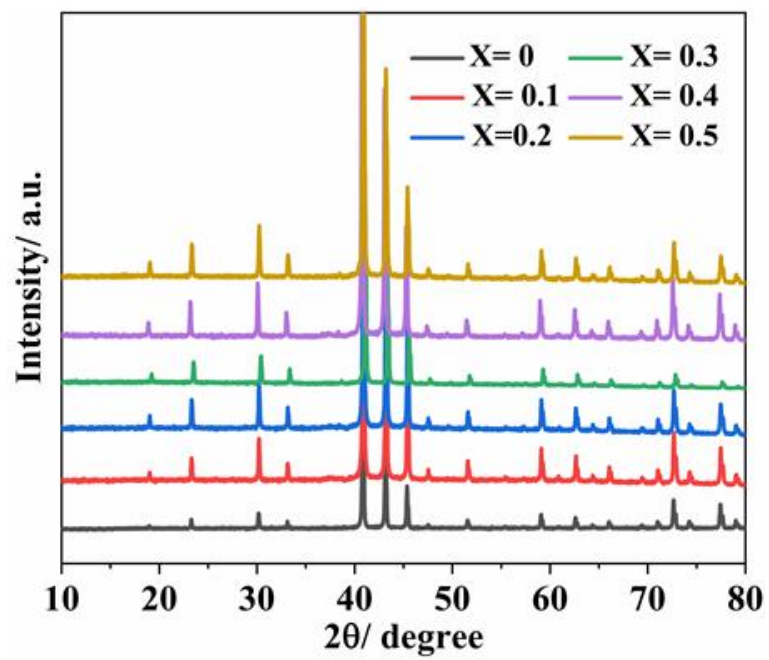


Fig. S11 XRD patterns for $\text{Ni}_2\text{W}_x\text{Mo}_{3-x}\text{N}$ ($x = 0.0, 0.1, 0.2, 0.3, 0.4$ and 0.5) samples heated under NH_3 at 800°C for 12 h.

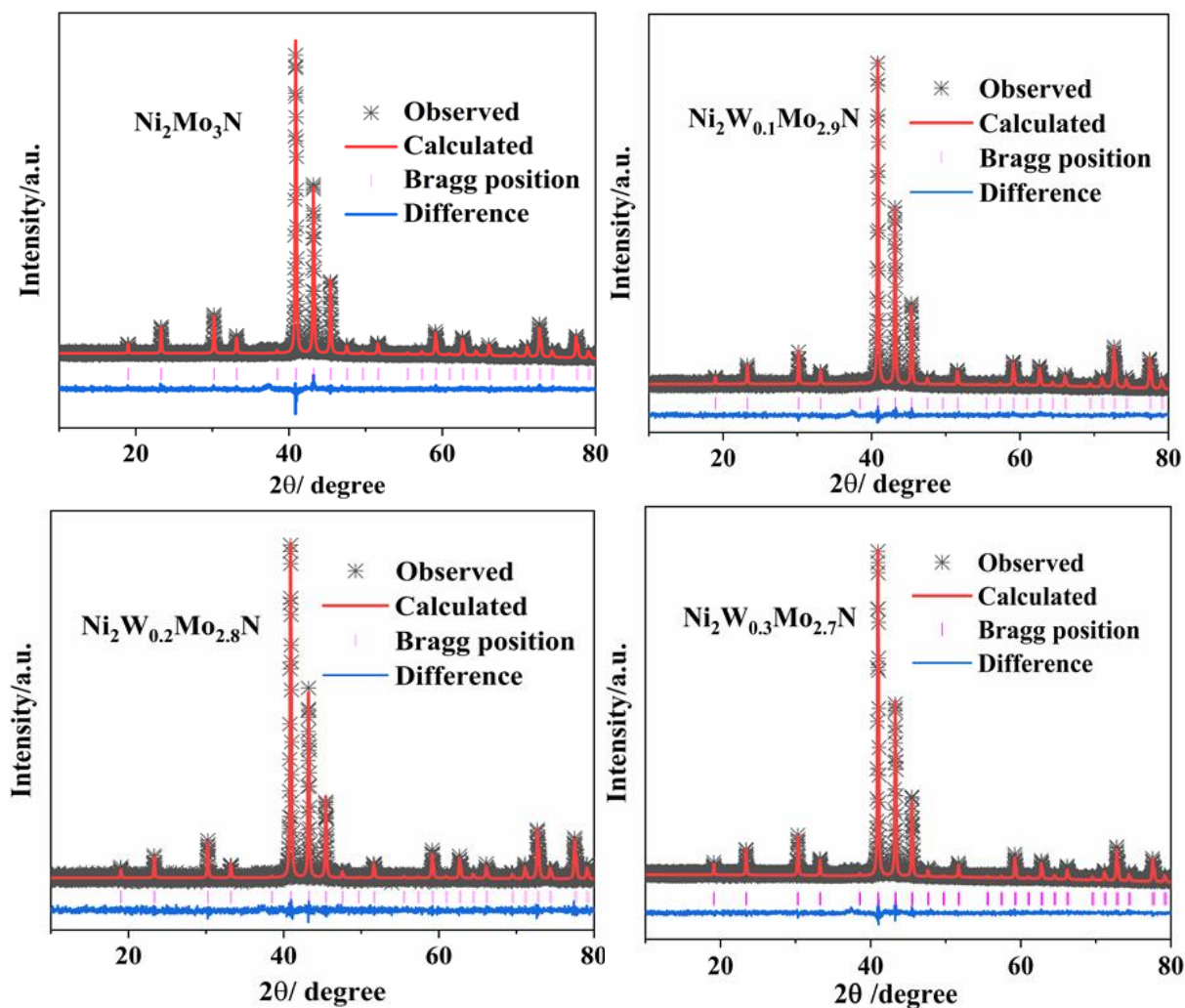


Fig. S12 Rietveld fits to the XRD patterns of $\text{Ni}_2\text{Mo}_3\text{N}$ ($R_{\text{wp}}\% = 4.9$ and $R_{\text{p}}\% = 3.9$), $\text{Ni}_2\text{W}_{0.1}\text{Mo}_{2.9}\text{N}$ ($R_{\text{wp}}\% = 4.9$ and $R_{\text{p}}\% = 3.9$), $\text{Ni}_2\text{W}_{0.2}\text{Mo}_{2.8}\text{N}$ ($R_{\text{wp}}\% = 4.9$ and $R_{\text{p}}\% = 3.9$) and $\text{Ni}_2\text{W}_{0.3}\text{Mo}_{2.7}\text{N}$ ($R_{\text{wp}}\% = 4.9$ and $R_{\text{p}}\% = 3.9$). Black crosses mark the data points, the red continuous line the fit and the blue continuous line the difference. Pink tick marks show the positions of the allowed reflections for the filled β - manganese structure $\text{Ni}_2\text{W}_x\text{Mo}_{3-x}\text{N}$ series with space group $P4_132$.

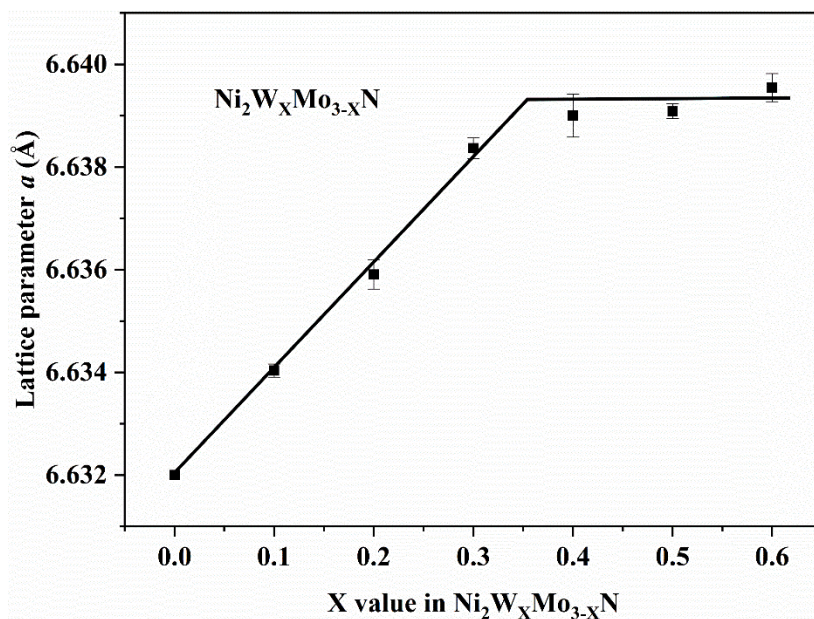


Fig. S13 Lattice parameter variation with tungsten content for $\text{Ni}_2\text{W}_x\text{Mo}_{3-x}\text{N}$ samples, showing the limit of tungsten solubility at around $x = 0.3$.

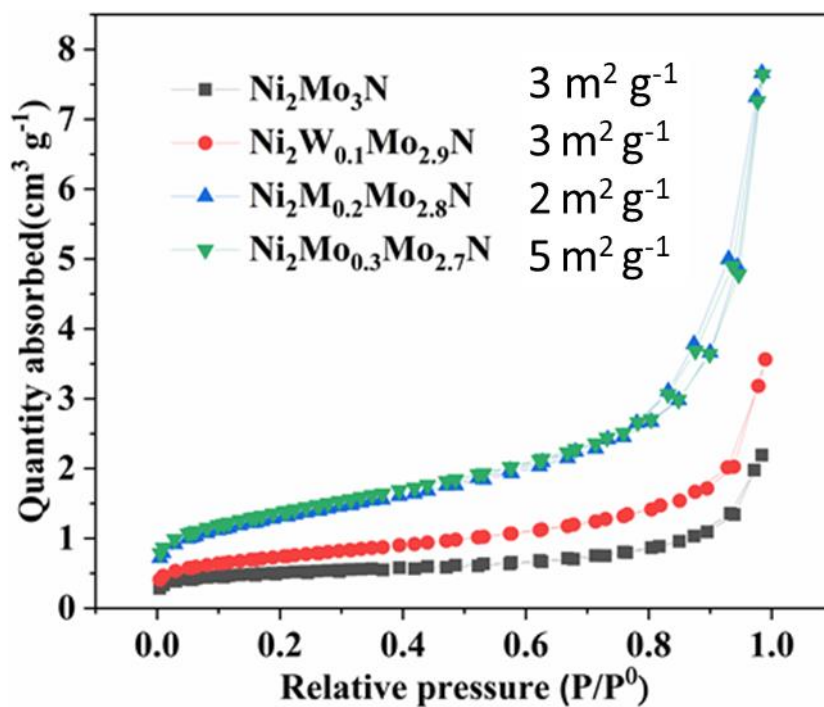


Fig. S14 Nitrogen adsorption/desorption isotherms curves for the $\text{Ni}_2\text{W}_x\text{Mo}_{3-x}\text{N}$ samples.

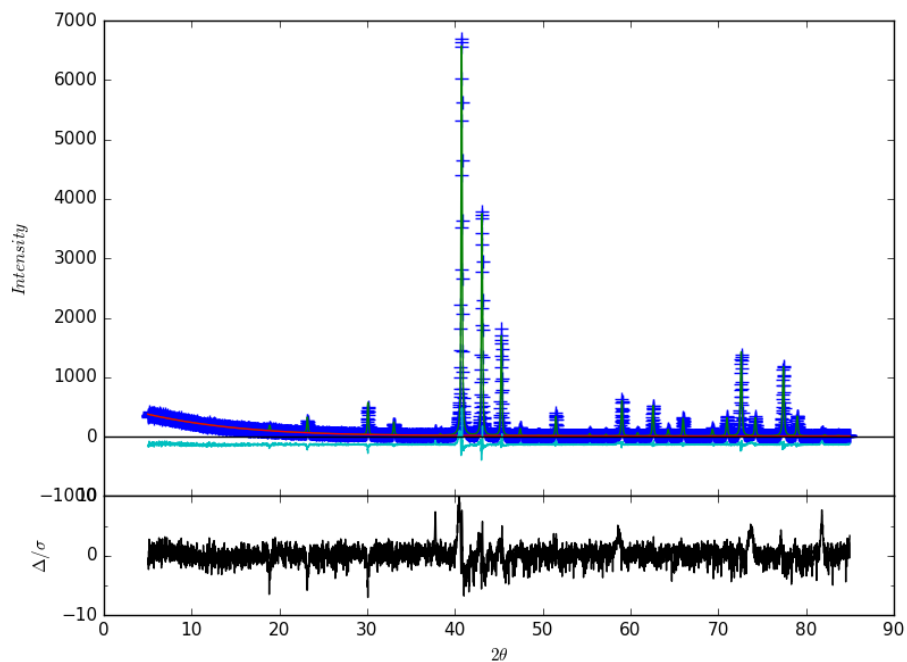


Fig. S15 Fit in $P4_132$ to the XRD data for $\text{Ni}_2\text{Mo}_3\text{N}$ after reduction treatment with H_2/Ar . In the upper plot blue crosses mark the data points, green lines the fit, cyan the difference and the red line the background. The lower plot is an expansion of the difference line. $R_{\text{wp}} = 14.5\%$, $a = 6.63209(13) \text{ \AA}$; Mo $x = 0.20196(13)$, $y = 0.45196(13)$, $z = 0.125$, $U_{\text{iso}} = 0.0103(5)$; Ni $x = y = z = 0.0668(2)$, $U_{\text{iso}} = 0.0099(9)$; N $x = y = z = 0.375$, $U_{\text{iso}} = 0.025$.

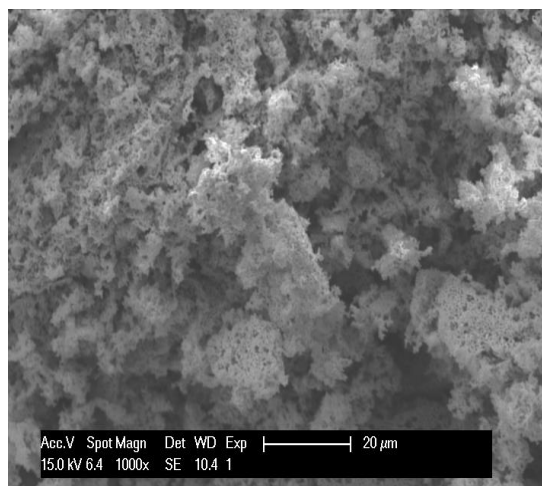


Fig. S16 Representative SEM image of $\text{Ni}_2\text{Mo}_{2.7}\text{W}_{0.3}\text{N}$ produced at 800°C .

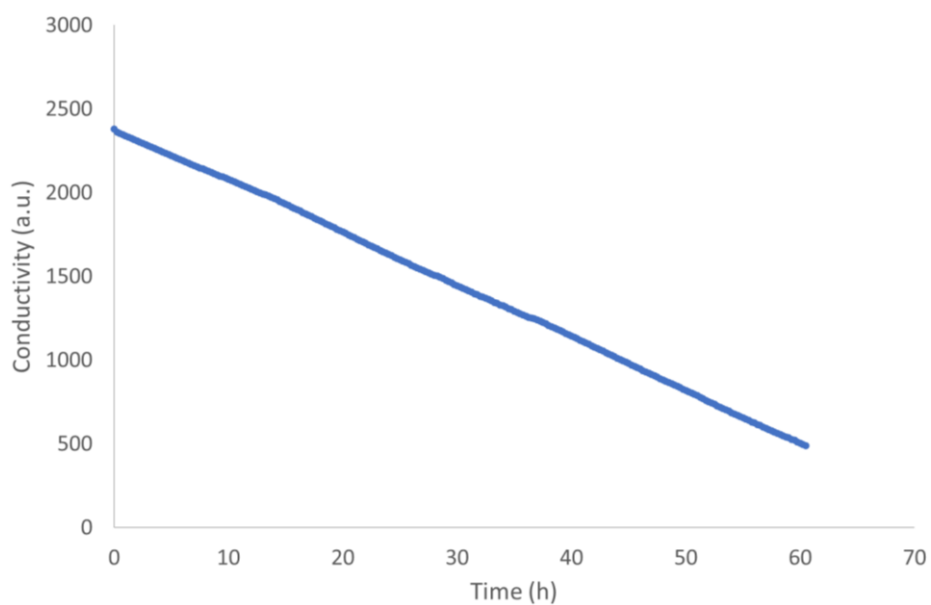


Fig. S17 Reaction profile of $\text{Ni}_2\text{Mo}_{2.8}\text{W}_{0.2}\text{N}$ under 3:1 H_2/N_2 at 400°C for 60.5 h. Conductivity relates to that of aqueous sulfuric acid solution through which the reactor effluent is flowed. Decreasing conductivity corresponds to ammonia production wherein H^+ ions react with NH_3 to form NH_4^+ ions.

	Co₃Mo₃N	Co₃W_{0.1}Mo_{2.9}N	Co₃W_{0.2}Mo_{2.8}N	Co₃W_{0.3}Mo_{2.7}N	Co₃W_{0.4}Mo_{2.6}N
Co 32e <i>x, x, x</i>					
<i>x</i>	0.2917(3)	0.290373(5)	0.29111(4)	0.290993(4)	0.29127(3)
U_{iso}	0.3377(3)	0.029683(3)	0.03739(3)	0.01568(4)	0.0257 (3)
Co 16d 1/2, 1/2, 1/2					
U_{iso}	0.03125	0.019074(5)	0.0267(5)	0.00176(4)	0.32489 (2)
W/Mo 48f <i>x, 1/8, 1/8, 1/8</i>					
<i>x</i>	0.32513(3)	0.324154(3)	0.324854(3)	0.32418(3)	0.32489 (2)
U_{iso}	0.3697 (1)	0.02212(2)	0.0238 (1)	0.00886(1)	0.02499 (1)
N 16c 0,0,0 U_{iso}	0.025				

Table S1 Atomic parameters of Co₃W_xMo_{3-x}N (*x* = 0.0, 0.1, 0.2, 0.3 and 0.4) obtained from XRD refined data.

	Co₃W_{0.5}Mo_{2.5}N	Co₃W_{0.6}Mo_{2.4}N	Co₃W_{0.7}Mo_{2.3}N	Co₃W_{0.8}Mo_{2.2}N
Co 32e <i>x, x, x</i>				
<i>x</i>	0.291759(4)	0.290684(4)	0.291809(4)	0.29037(4)
U_{iso}	0.02448(3)	0.0325(3)	0.02546(3)	0.02287(3)
Co 16d 1/2, 1/2, 1/2				
U_{iso}	0.01538(4)	0.03249(4)	0.01795(4)	0.02344(2)
W/Mo 48f <i>x, 1/8, 1/8, 1/8</i>				
<i>x</i>	0.3256(3)	0.324849(2)	0.325296(2)	0.325325 (2)
U_{iso}	0.02769(1)	0.03196 (1)	0.03081(1)	0.01786 (1)
N 16c 0,0,0 U_{iso}	0.025			

Table S2 Atomic parameters of Co₃W_xMo_{3-x}N (*x* = 0.5, 0.6, 0.7 and 0.8) obtained from XRD refined data.

x in $\text{Co}_3\text{W}_x\text{Mo}_{3-x}\text{N}$	$a/\text{\AA}$	$R_{\text{wp}}, R_p/\%$	Crystallite size/ nm
0	11.024(4)	3.9, 3.13	94(5)
0.1	11.02337(5)	4.89, 3.86	97(7)
0.2	11.02322(5)	4.86, 3.88	133(12)
0.3	11.02218(5)	4.87, 3.88	199(33)
0.4	11.02104(5)	4.73, 3.78	159(14)
0.5	11.02006(5)	4.86, 3.85	133(11)
0.6	11.01935(5)	5.03, 4.01	114(8)
0.7	11.01872(4)	5.27, 4.18	114(8)
0.8	11.01741(4)	5.18, 4.08	114(8)

Table S3 Crystallographic information obtained from Rietveld refinement of $\text{Co}_3\text{W}_x\text{Mo}_{3-x}\text{N}$ samples.

Element	$\text{Co}_3\text{W}_{0.4}\text{Mo}_{2.6}\text{N}$	
	Expected	Actual
Co	42.9	40.6
W	5.7	3
Mo	42.9	54

Table S4 The atom percentage of the $\text{Co}_3\text{W}_{0.4}\text{Mo}_{2.6}\text{N}$ sample evaluated by EDX analysis.

Composition	a/Å	R _{wp} , R _p / %	Crystallite size/ nm	Ni 8c (x, x, x)		W/Mo 12 d (1/8, y, z)			N 4a 3/8, 3/8,3/8
				x	U _{iso} / Å ²	y	Z	U _{iso} / Å ²	U _{iso} / Å ²
Ni ₂ Mo ₃ N	6.632(2)	11.9, 9.24	114(5)	0.067284(3)	0.0674(2)	0.2017(2)	0.4517(2)	0.03105(9)	0.2500
Ni ₂ W _{0.1} Mo _{2.9} N	6.63404(2)	7.3, 5.64	104(9)	0.066204(3)	0.02926(1)	0.2018(2)	0.4518(2)	0.03012(1)	
Ni ₂ W _{0.2} Mo _{2.8} N	6.6359(2)	11.52, 8.83	89(7)	0.067084(5)	0.0144(2)	0.201793 (3)	0.451793(3)	0.01644(1)	
Ni ₂ W _{0.3} Mo _{2.7} N	6.63837(2)	8.22, 6.34	80(3)	0.067536(3)	0.05186(2)	0.201897(2)	0.4519(2)	0.04713(1)	

Table S5 Atomic parameter and crystallographic information obtained from Rietveld refinement of Ni₂W_xMo_{3-x}N (x = 0.0, 0.1, 0.2 and 0.3) samples.

In a series of different measurements, the ammonia synthesis activity was tested using 0.15 g of material. First, the nitrides were pre-treated at 700°C for 2 hours with 3:1 H₂/N₂ (BOC, H₂ 99.998 %, N₂ 99.995 %) at a total gas feed of 12 mL min⁻¹. The ammonia synthesis rates were then measured at atmospheric pressure and 500°C under the same gas flow.

Material	Specific Activity (μmol h ⁻¹ m ⁻²)
Co ₃ Mo ₃ N	113 ± 5
Co ₃ Mo _{2.9} W _{0.1} N	103 ± 6
Co ₃ Mo _{2.8} W _{0.2} N	103 ± 8
Co ₃ Mo _{2.6} W _{0.4} N	98 ± 5
Ni ₂ Mo ₃ N	143 ± 13
Ni ₂ Mo _{2.9} W _{0.1} N	140 ± 8
Ni ₂ Mo _{2.8} W _{0.2} N	94 ± 2
Ni ₂ Mo _{2.7} W _{0.3} N	91 ± 3

Table S6 Ammonia synthesis activity under 3:1 H₂/N₂ (12 mL min⁻¹) at 500 °C.